

The spectroscopy of solar sterile neutrinos

Ilídio Lopes ^{1,2,a}

¹Centro de Astrofísica e Gravitação - CENTRA, Departamento de Física, Instituto Superior Técnico - IST, Universidade de Lisboa - UL, Av. Rovisco Pais 1, 1049-001 Lisboa, Portugal

²Institut d'Astrophysique de Paris (UMR 7095: CNRS & UPMC, Sorbonne Universités), 98 bis Bd Arago, F-75014 Paris, France

the date of receipt and acceptance should be inserted later

Abstract We predict the sterile neutrino spectrum of some of the key solar nuclear reactions and discuss the possibility of these being observed by the next generation of solar neutrino experiments. By using an up-to-date standard solar model with good agreement with current helioseismology and solar neutrino flux data sets, we found that from solar neutrino fluxes arriving on Earth only 3%-4% correspond to the sterile neutrino. The most intense solar sources of sterile neutrinos are the pp and ${}^7\text{Be}$ nuclear reactions with a total flux of $2.2 \times 10^9 \text{ cm}^2\text{s}^{-1}$ and $1.8 \times 10^8 \text{ cm}^2\text{s}^{-1}$, followed by the ${}^{13}\text{N}$ and ${}^{15}\text{O}$ nuclear reactions with a total flux of $1.9 \times 10^7 \text{ cm}^2\text{s}^{-1}$ and $1.7 \times 10^7 \text{ cm}^2\text{s}^{-1}$. Moreover, we compute the sterile neutrino spectra of the nuclear proton-proton nuclear reactions – pp , hep and ${}^8\text{B}$ and the carbon-nitrogen-oxygen – ${}^{13}\text{N}$, ${}^{15}\text{O}$ and ${}^{17}\text{F}$ and the spectral lines of ${}^7\text{Be}$.

Keywords Neutrinos – Sun:evolution –Sun:interior – Stars: evolution –Stars:interiors

1 Introduction

The standard neutrino flavour oscillation model with only three neutrinos has been very successful in explaining most of observational properties of neutrino fluxes. Nevertheless, the significant improvement on the experimental methods of neutrino detection during the past fifteen years have revealed the existence of disagreements between the standard model of neutrino oscillations and experimental data. These discrepancies usually referred to as *neutrino anomalies* have been reported in a number of different type of experiments: the Liquid Scintillator Neutrino Detector (LSND; Aguilar

et al., 2001), the Booster Neutrino Experiment, (Mini-BooNE (first phase of BooNE); Aguilar-Arevalo et al., 2010, 2013), reactor experiments (Mention et al., 2011) and the gallium experiments (Giunti & Laveder, 2011). Several generalizations of the standard neutrino flavour oscillation model have been proposed in the literature to explain these neutrino anomalies (e.g., Gonzalez-Garcia & Maltoni, 2008; Maltoni & Smirnov, 2016). Among other solutions the most successful one is the prediction of the existence of a new type of neutrinos (Maki et al., 1962), known as *sterile neutrinos*. However, this experimental hint that can be explained by the existence of sterile neutrinos has been challenged by more recent measurements made by the NEOS Experiment (Ko et al., 2017), the Super-Kamiokande detector (Abe et al., 2015) and the IceCube Collaboration (Aartsen et al., 2017). Although the parameter space that allows the sterile neutrinos to explain the neutrino anomalies has been significantly reduced, their existence can still be accommodated within the current set of observations.

Sterile neutrinos are very well-motivated elementary particles and can be obtained from a trivial extension of the standard model of particle physics ¹. Their name reflects the fact that by definition sterile neutrinos are not affected by any of the known forces of nature except gravity, since these particles carry no charges and are singlets under all gauge groups of the standard model. This type of neutrinos, unlike other particle candidates, provides an unified description of three major problems in the framework of the standard model: the origin of the neutrino masses and the flavour oscillation

¹In the remainder of the article, the standard model will always refer to the standard model of particle physics if not stated otherwise.

^ae-mail: ilidio.lopes@tecnico.ulisboa.pt

model (Adhikari et al., 2017), the absence of primordial anti-matter in the Universe and the existence of dark matter (Boyarsky et al., 2012). Although many of the properties of this class of neutrinos is fixed by the generalized standard model, other properties of sterile neutrinos remain undefined, like their masses. Actually, all sorts of theoretical arguments have been proposed to explain the existence of sterile neutrinos with a very large range of mass scales: from neutrinos with very light masses much smaller than eV (de Holanda & Smirnov, 2004) up to very heavy neutrinos with masses of 10^{16} GeV (Minkowski, 1977). In recent years, particular attention has been dedicated to the sterile neutrino candidates with masses of a few eV, hundred keV and a few GeV (Shrock, 1980) as several experiments are already obtaining data or are under construction with the goal of probing the existence of sterile neutrinos on these mass ranges.

The exact number of sterile neutrinos is not known, but even the simplest of the neutrino flavour oscillation models in which only one extra sterile neutrino ν_s is added up to the standard active neutrinos (ν_e, ν_τ, ν_μ) is able to resolve many of the known experimental discrepancies – the neutrino anomalies. This model is the so-called 3+1 neutrino flavour oscillation model in which the generalized mass matrix leads to the mixing of 4 neutrinos ($\nu_e, \nu_\tau, \nu_\mu, \nu_s$). This basic model presents very compelling results compatible with experimental data (Billard et al., 2015; Palazzo, 2011). Following the literature (e.g., Billard et al., 2015), in our study we will focus on the 3+1 sterile neutrino in which two additional parameters are included to characterize the sterile neutrino flavour oscillations: the mass spilling $|\Delta m_{41}^2|$ and the mixing angle θ_{14} .

The mass spilling and the mixing angle (as defined in the 3+1 flavour neutrino oscillation model) that have been estimated by different research groups using several observational data sets and different fitting techniques, found very similar values for both quantities. A global analysis of the neutrino oscillation data in the 3+1 parameter space made by Giunti et al. (2013) found that Δm_{41}^2 could take a value between 0.82–2.19 eV^2 at 99.7% confidence level. Similarly, Ko et al. (2017) making an independent analysis have obtained identical values for $|\Delta m_{41}^2|$, specifically mass values in the range 0.2 – 2.3 eV^2 . The determination of θ_{14} by different research groups leads also to similar values. For instance, Billard et al. (2015) and Ko et al. (2017), found for the upper limit of θ_{14} the values: $10.6^\circ(0.1855)$ and $9.2^\circ(0.1582)$. These values for θ_{14} differ only slightly from the first determination made by Palazzo (2011) that found $11.7^\circ(0.204)$. Conveniently, for our calculations we choose for the fiducial value of

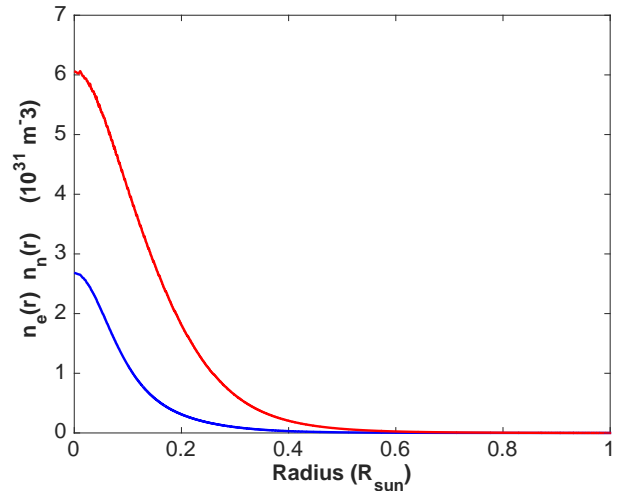


Fig. 1 The plasma of the Sun's core is made of ions and free electrons. The plot shows the variation of the number density of electrons $n_e(r)$ (red curve) and neutrons $n_n(r)$ (blue curve). In the computation of this quantities we used the solar standard model which is in excellent agreement with the helioseismic data. See Lopes & Silk (2013) for details.

θ_{14} the most recent determined value: $9.2^\circ(0.1582)$ or $\sin^2(2\theta_{14}) = 0.1$ (Ko et al., 2017).

Since sterile neutrinos do not take part in the weak interaction, the most obvious way to observe their effect is via their mixing with the active neutrinos. Therefore, with the goal of determining the sterile neutrino properties, in this study we predict the spectra of sterile and electron neutrinos coming from the Sun, on the hope this will contribute to their discovery by "direct" detection by one of the ongoing experiments, the ultimate silver bullet that will prove their existence. Specifically, we compute the sterile neutrino and electron neutrino spectra of some of the key nuclear reactions occurring in the Sun's core. These two types of neutrino spectra, as we will discuss in this work, results from the conversion of electron neutrinos into sterile neutrinos and from the survival of electron neutrinos, due to their oscillation between the 4 neutrino flavours, as these particles propagate through space (vacuum and matter). Specifically, we predict the shape of the different solar sterile and electron neutrino spectra of the key neutrino nuclear reactions of the proton-proton (PP) chain and carbon-nitrogen-oxygen (CNO) cycle occurring in the interior of the present Sun. The calculation will be made for the current solar standard model which used the most up-to-date physics (equation of state, opacities, nuclear reactions rates and microscopic diffusion of heavy elements). The details about the physics of the solar model used in this study can be found in Lopes & Silk (2013); Lopes & Turck-Chièze (2013). This so-

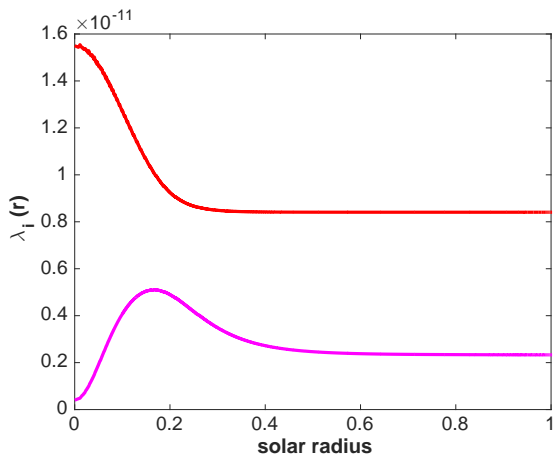


Fig. 2 The level crossing scheme: The mass eigenvalues λ_1 (red curve) and λ_2 (magenta curve) as a function of the solar radius (cf. equation 1). These λ values correspond to a neutrino with an energy $E = 3.5 \text{ MeV}$.

lar model predicts the sound speed profile and solar neutrino fluxes in agreement with observational data and similar to other models found in the literature (i.e., Turck-Chièze et al., 2010; Serenelli et al., 2011).

In the next section, we discuss in some detail the 3+1 sterile neutrino flavour oscillation model. In the following section, we present the spectra predictions for sterile and electron neutrinos of several of the key solar nuclear reactions. In the last section, we discuss the results and their implications for the next generation of sterile neutrino experiments.

2 Neutrino flavour oscillation models

This study focuses on the simple and popular 3 + 1 neutrino flavour oscillation model with 4 neutrinos: ν_e , ν_μ , ν_τ and ν_s . The addition of an extra (sterile) neutrino leads to a new flavour oscillation component on the 3 + 1 neutrino model defined by a new mass splitting $|\Delta m_{41}^2|$ and a new mixing angle θ_{14} . As discussed previously, a recent fit of the experimental data to the 3+1 neutrino model done by Billard et al. (2015) found $\sin^2 \theta_{14} = 0.034$ (or $\theta_{14} \sim 10.6^\circ(0.1855)$), $\Delta m_{21}^2 = (7.5 \pm 0.14) \times 10^{-5} \text{ eV}^2$, $\sin^2(\theta_{12}) = 0.300 \pm 0.016$ and $\sin^2 \theta_{13} = 0.03$. In our calculations of the 3+1 neutrino oscillation model we will use these parameters. However the value of θ_{14} is replaced by a recent estimation of $9.2^\circ(0.1582)$ obtained by Ko et al. (2017). This choice of θ_{14} does not change our conclusions since the difference between the two values is small to affect our results. It is important to highlight that the experimental data used by Billard et al. (2015) for the previous

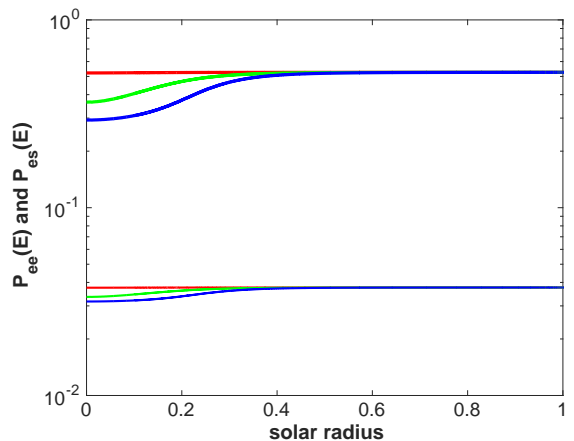


Fig. 3 The neutrino probability functions: $P_{es}(E)$ corresponds to the probability of conversion of ν_e to ν_s neutrinos given by equation 2 (bottom set of curves); and $P_{ee}(E)$ corresponds to the survival probability of ν_e given by equation 3 (top set of curves). The red, green and blue curves correspond to neutrinos with energy of 0.1, 5 and 15 MeV, which correspond to typical values of neutrino energies produced inside the Sun's core. In the computation of these quantities we used the standard solar model (see Lopes & Silk (2013) for details).

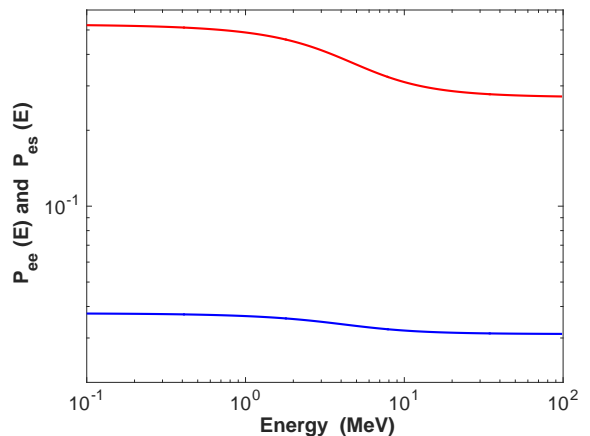


Fig. 4 The neutrino probability functions as a function of the neutrino energy: $P_{es}(E)$ corresponds to the probability of conversion of ν_e to ν_s neutrinos (blue curve); $P_{ee}(E)$ corresponds to the survival probability of ν_e neutrinos (red curve). See Figure 3 for details.

fits comprises data from solar detectors like SNO, Super Super-Kamiokande, Borexino, Homestake, and Gallium experiments and reactors data from the very long baseline KamLAND. Effectively, the inclusion of more experimental data, like the data sets coming from short baseline detectors such as the DAYA-BAY, RENO, and Double Chooz reactor experiments changes only slightly the value of $\sin^2 \theta_{14}$ and once again its magnitude variation is too small to significantly affect our results and conclusions (Billard et al., 2015). Actually, although

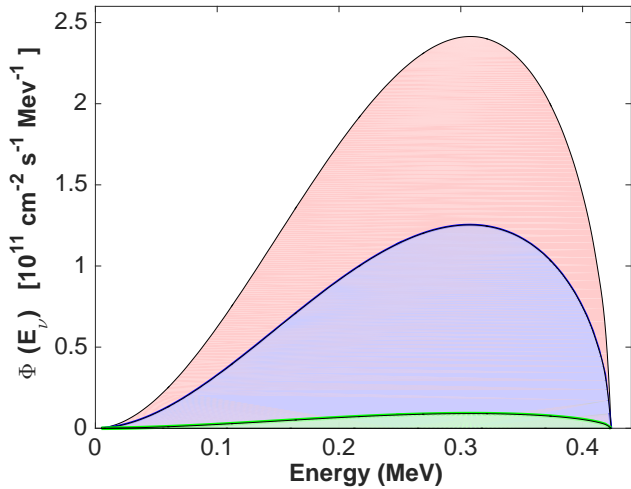


Fig. 5 Neutrino spectrum of pp nuclear reaction: the $\Phi_t(E)$ (red area) is the electron neutrino spectrum inside the Sun. $\Phi_{ee}^{\odot}(E)$ (blue area) and $\Phi_{es}^{\odot}(E)$ (green area) are the survival electron and sterile solar neutrino spectra for the PP neutrinos 3 + 1 neutrino flavour oscillation model.

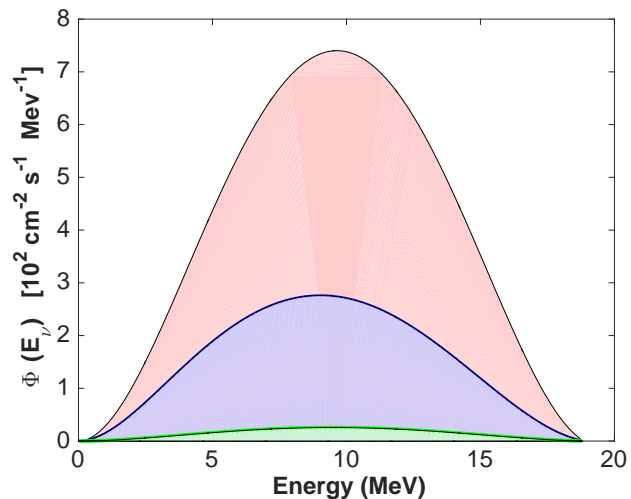


Fig. 6 Neutrino spectrum of hep nuclear reaction. The colour scheme is the same used in Figure 5.

$\sin^2 \theta_{14}$ has changed over the years, its present value is only slightly different from the value originally found by Palazzo (2011): $\sin^2 \theta_{14} = 0.041$. Moreover, we observe that the $|\Delta m_{41}^2|$ determined by Ko et al. (2017) to be in the mass range of $\sim 0.2 - 2.3 eV^2$ is much larger than the mass splittings, $|\Delta m_{21}^2|$ and $|\Delta m_{32}^2|$ estimated to be of the order of $10^{-5} eV^2$ and $10^{-3} eV^2$ (Ko et al., 2017; Gonzalez-Garcia et al., 2016). We note that in the 3+1 neutrino model discussed in our study only the mixing angle θ_{14} is considered to have a value different from zero (Billard et al., 2015; Palazzo, 2011). We stress this is a very good approximation, since a fit to the

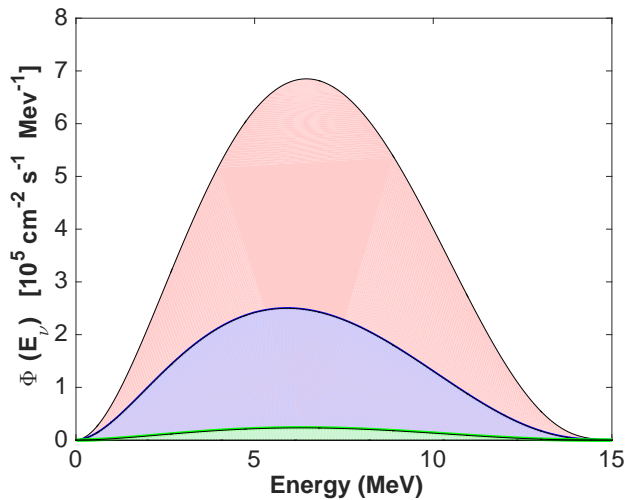


Fig. 7 Neutrino spectrum of 8B nuclear reaction. The colour scheme is the same used in Figure 5.

3+1 neutrino model (with more mixing angles), that besides the new mixing angle θ_{14} also has additional mixing angles like θ_{24} and θ_{34} (associated with other possible flavour oscillations), found relatively small values for θ_{24} and θ_{34} (Kopp et al., 2013). Therefore setting these last mixing angles to zero will not affect our results and conclusions. The experimental facts discussed above justify the analytical neutrino oscillation model that we will discuss in the next subsection.

Finally, we point out that our 3 + 1 neutrino model has parameters (excluding Δm_{41} and θ_{41}) very similar to the ones found for the standard 3 neutrino flavour oscillation model. For reference, a recent estimation of parameters made by Gonzalez-Garcia et al. (2016) using the standard 3 flavour neutrino oscillation model to fit the combined experimental data set obtained from atmospheric experiments, solar detectors and particle accelerators found the following set of parameters: $\Delta m_{31}^2 \sim 2.457 \pm 0.045 \cdot 10^{-3} eV^2$ (or $\sim -2.449 \pm 0.048 \cdot 10^{-3} eV^2$), $\Delta m_{21}^2 \sim 7.500 \pm 0.019 \cdot 10^{-5} eV^2$, $\sin^2 \theta_{12} = 0.304 \pm 0.013$, $\sin^2 \theta_{13} = 0.0218 \pm 0.001$, $\sin^2 \theta_{23} = 0.562 \pm 0.032$ and $\delta_{CP} = 2\pi/25 n$ with $n = 1, \dots, 25$. This set of parameters of values is also confirmed by other authors (Gonzalez-Garcia et al., 2014; Bergström et al., 2015).

2.1 The standard and 3+1 neutrino flavour models

The neutrino oscillation model with a fourth sterile neutrino ν_s is such that the neutrino flavours ($\nu_e, \nu_\mu, \nu_\tau, \nu_s$) and the mass eigenstates ($\nu_1, \nu_2, \nu_3, \nu_4$) are connected through a 4×4 unitary mixing matrix U . We choose for U the parametrization proposed by Palazzo (2011)

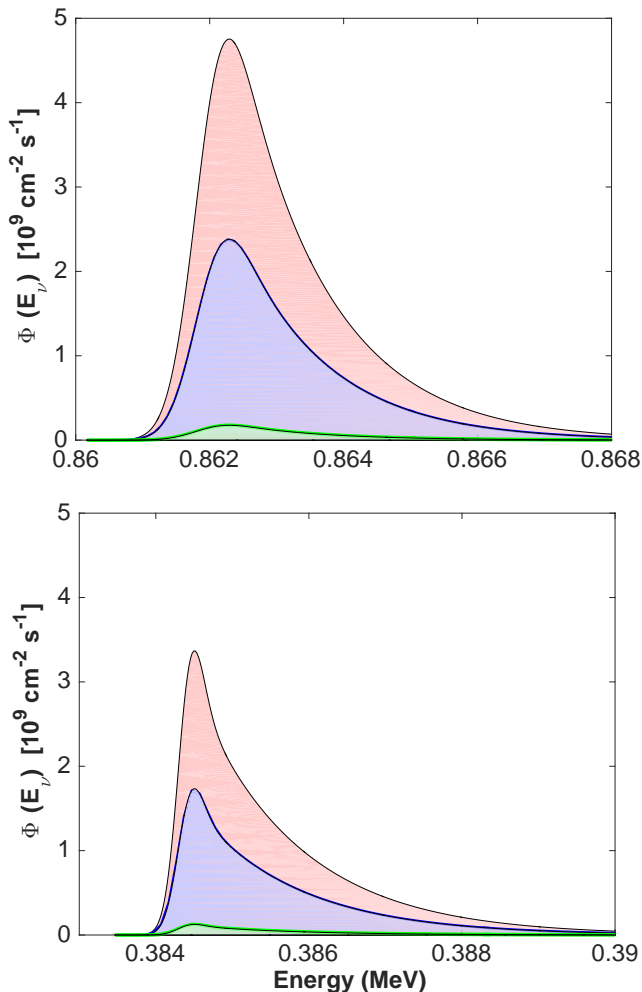


Fig. 8 Neutrino of the two line spectra of ${}^7\text{Be}$ nuclear reaction. The colour scheme is the same used in Figure 5.

which is optimized to study the solar neutrino sector. It is worth highlighting that this peculiar parametrization is somehow between an admixture of flavour eigenstates and matter eigenstates, as discussed by Cirelli et al. (2005). Such U formulation ensures this 3+1 neutrino model has the required sensitivity to the flavour-type and mass-type admixtures needed to study the solar data sector. In particular, this 3+1 mixing matrix is such that the standard neutrino model corresponds to $\theta_{14} = 0$. A detailed account of the properties of this model can be found in Palazzo (2011). In particular, the electron neutrino ν_e oscillation with the (ν_1, ν_2) mass eigenstates is only slightly affected by the decoupled (ν_3, ν_4) mass eigenstates for which the associated mixing angles are very small. In such neutrino model, the MSW effect is computed in the hierarchical limit $\Delta m_{21}^2/2E \ll \Delta m_{31}^2/2E \ll \Delta m_{41}^2/2E$ where E is the energy of the neutrino, an $\Delta m_{i1}^2 = m_i^2 - m_1^2$ where m_i

is the mass of each neutrino. This 3+1 neutrino model is an obvious generalisation of the standard (3 active) neutrino model (Kuo and Pantaleone, 1989). In both cases neutrino oscillations are approximated by an effective 2 neutrino oscillation model. As a consequence the ν_3 and ν_4 evolve independent of each other and completely independent of the doublet: (ν_1, ν_2) .

2.2 The eigenvalues of the mass matrix in 3+1 model

In the Sun, as the experimental data on neutrino fluxes is limited, it is sufficient to represent the survival or conversion of neutrino flavor, using a two neutrino flavour oscillation model (Kuo and Pantaleone, 1989). The neutrinos emitted by the solar nuclear reactions are typically of low energy, since these neutrinos have always an energy smaller than 20 MeV. Accordingly, some of the properties of solar neutrinos can be well understood by means of a two active neutrino flavour model: one electron neutrino ν_e and a second active neutrino, which we choose to be ν_μ , since the ν_τ mixing angle is very small. Another way to interpret this approximation, is to assume that ν_μ now means the generic active $\nu_{\mu\tau}$, if not stated otherwise. In this much simpler 2 (active)+1 (sterile) neutrino flavour model (ν_e, ν_μ, ν_s) , the properties of the sterile neutrino ν_s can be computed as an approximation to the $(\nu_e, \nu_\mu, \nu_\tau, \nu_s)$ neutrino model. Accordingly, this 2+1 neutrino model has the following active mass eigenstates ν_1 and ν_2 , as well as a sterile mass eigenstate² ν_4 (de Holanda & Smirnov, 2004; Cirelli et al., 2005). The 2+1 flavour model in the absence of sterile neutrinos have the following eigenvalue expressions (de Holanda & Smirnov, 2004). If λ_i ($i = 1, 2$) are the correspondent eigenvalues of the mass matrix, it reads

$$\lambda_i = \frac{M^2}{4E} + \frac{V_e + V_n}{2} \mp \sqrt{\left(\Delta_c - \frac{V_e - V_n}{2}\right)^2 + \Delta_s^2}, \quad (1)$$

where $M^2 = m_1^2 + m_2^2$, $\Delta_c \equiv \Delta m_{21}^2 \cos(2\theta_{21})/(4E)$ and $\Delta_s \equiv \Delta m_{21}^2 \sin(2\theta_{12})/(4E)$, $V_e = \sqrt{2}G_F(n_e - n_n/2)$ and $V_n = -\sqrt{2}G_F n_n/2$, where G_F is the Fermi constant and $n_e(r)$ and $n_n(r)$ are the profile of electron and neutron densities of the solar interior. The electron density $n_e(r)$ is given by $N_o \rho(r)/\mu_e(r)$, where $\mu_e(r)$ is the mean molecular weight per electron, $\rho(r)$ is the density of matter in the solar interior, and N_o is Avogadro's number. The density of neutrons $n_n(r)$ is computed in

²The option to use the subscript 4 for the mass eigenstate of the sterile neutrino is motivated by the fact of maintaining a simple correspondence between the 2+1 and 3+1 neutrino flavour models.

a similar manner like $n_e(r)$ where the mean molecular weight per electron $\mu_e(r)$ is replaced by the mean molecular weight per neutron $\mu_n(r)$.

Figure 1 shows the current abundances of electrons and neutrons inside the Sun (as a function of the solar radius) for its present age as predicted by an up-to-date standard solar model (Lopes & Silk, 2013). The large amount of $n_n(r)$ in the center of the Sun results from the fact that the Sun's core is made of more than 70% of ${}^4\text{He}$. This occurs as a result of this element being continuously produced (nucleosynthesis) by the conversion of 4 protons (0 neutrons) into an ion of ${}^4\text{He}$ (2 neutrons). This process has been occurring since our star arrived to the main sequence 4.5 Gyr ago and will continue to do it for the next 5 Gyr (until the Sun leaves the main sequence). As a consequence, at the present age the core of the Sun has a larger amount of neutrons than the more external layers, leading to a decrease of $n_n(r)$ from the center towards the surface of the star. This important point is illustrated in Figure 1 where we show for electrons and neutrons the relative density and mean molecular weight per particle inside the Sun.

For illustrative purposes we assume that $m_i^2 \approx \Delta m_{i1}^2$ (with $i \neq 1$). Specifically, $m_1^2 \approx 0$, $m_2^2 \approx 7.5 \times 10^{-5} \text{ eV}^2$ (with $\theta_{12} \approx 0.6$), $m_3^2 \approx 2.4 \times 10^{-3} \text{ eV}^2$ (with $\theta_{13} \approx 0.13$), and $m_4^2 \approx 1.0 \text{ eV}^2$ (with $\theta_{14} \approx 0.16$). The λ_i ($i = 1, 2$) can be seen in the figure 2. In this model for which $m_1 < m_2 < m_3 < m_4$, there is only a relevant resonance in the system associated with 1-2 level crossing. The 1-2 resonance energy is given by the expression $E_{12} = \Delta m_{21}^2 \cos(2\theta_{12}) / (2\sqrt{2}G_F n_e)$. As the electron neutrino moves outward, the electronic density decreases and the neutrino eventually go through the resonance region $E_{12}(r)$ and beyond. However, since the electron density $n_e(r)$ in the Sun's core varies slowly, i.e., $dn_e(r)/dr$ is small, the propagation is adiabatic, the neutrino state will remain in the same mass eigenstate, then the ν_e will emerge associated with ν_1 . The flavor composition of ν_2 is now determined by the mixing angle in the vacuum and the ν_2 is now mostly $\nu_{\mu\tau}$.

We notice that for other neutrino models the eigenvalues can have additional resonances. For instance, de Holanda & Smirnov (2004) have shown that for a 2+1 neutrino flavour model ($\nu_e, \nu_{\mu\tau}, \nu_s$) with $m_1 < m_4 < m_2$, the sterile neutrino level λ_4 crosses λ_1 . In this model, the λ_2 essentially decouples, therefore it is not affected by the s-mixing. However, in such a neutrino model, due to the variation of the $n_e(r)$ in the Sun's core, the eigenvalues have two resonances: one related with the active neutrinos, the 1-2, i.e., the same resonance mentioned previously; and a new resonance, the 1-4, that corresponds to λ_4 crosses λ_1 in a region at

the right of the 1-2 resonance³. However, this case does not occur in our study, since in our 2+1 model λ_4 is much larger than λ_1 and λ_2 and consequently does not cross any of them.

2.3 The conversion of sterile neutrino in electronic neutrinos

The goal of this work is to predict the spectra of sterile and electronic neutrinos emitted by the Sun for which their specific shapes strongly depend on the properties of the plasma of the solar interior. As such, in the following we start to compute the probabilities of conversion of electron neutrino to sterile neutrino P_{es} [$\equiv P(\nu_e \rightarrow \nu_s)$] arriving on Earth. Equally we also compute the survival probability of electron neutrino P_{ee} [$\equiv P(\nu_e \rightarrow \nu_e)$]. In this 3+1 neutrino flavour oscillation model like in the standard 3 flavour oscillations (e.g., Bilenky, 2010), the neutrino oscillates between the available flavours due to oscillations in vacuum and matter (Mikheyev-Smirnov-Wolfenstein (MSW), e.g., Wolfenstein, 1978). The survival and conversion probabilities of a four-flavour neutrino oscillation can be reduced to a modified three-flavour and two-flavour neutrino oscillation model. These simplifications results from the difference of magnitude between mass splittings and mixing angles. A detailed discussion about the neutrino flavour oscillation model can be found in Gonzalez-Garcia & Maltoni (2008).

Since the evolution of neutrinos in matter is adiabatic, for that reason their contribution for P_{es} and P_{ee} can be cast in simple expressions (Palazzo, 2011). Following, the usual parametrization of the neutrino mixing matrix this leads to the following expression for P_{es} (probability conversion from ν_e to ν_s):

$$P_{es} = s_{14}^2 c_{14}^2 c_{13}^4 \bar{P}_{ee}^{2\nu} + s_{14}^2 c_{14}^2 s_{13}^4 + s_{14}^2 c_{14}^2, \quad (2)$$

where $c_{ij} = \cos\theta_{ij}$ and $s_{ij} = \sin\theta_{ij}$. Equally the survival probability of electron neutrinos P_{ee} reads

$$P_{ee} = c_{14}^4 c_{13}^4 \bar{P}_{ee}^{2\nu} + c_{14}^4 s_{13}^4 + s_{14}^4. \quad (3)$$

In the previous equations $\bar{P}_{ee}^{2\nu}$ is the electron neutrino survival probability in a two-flavour neutrino oscillation model. It reads

$$\bar{P}_{ee}^{2\nu} = c_{12}^2 (c_{12}^m)^2 + s_{12}^2 (s_{12}^m)^2, \quad (4)$$

where θ_{12}^m is the matter angle that depends equally of the fundamental parameters of neutrino flavour oscillations and the properties of solar plasma. θ_{12}^m can be

³As explained by de Holanda & Smirnov (2004), in principle λ_4 could cross λ_1 twice: one above and another below the 1-2 resonance.

equally determined from one of the following expressions:

$$\cos(2\theta_{12}^m) = \frac{\cos(2\theta_{12}) - V_m(r)}{\sqrt{[\cos(2\theta_{12}) - V_m(r)]^2 + [\sin(2\theta_{12})]^2}}, \quad (5)$$

or

$$\sin(2\theta_{12}^m) = \frac{\sin(2\theta_{12})}{\sqrt{[\cos(2\theta_{12}) - V_m(r)]^2 + [\sin(2\theta_{12})]^2}}. \quad (6)$$

In the previous expressions $V_m(r)$ is the effective matter potential given by

$$V_m(r) = c_{13}^2 (c_{14}^2 + f_m(r)s_{14}^2) \frac{2E\sqrt{2}G_F n_e(r)}{\Delta m_{21}^2}. \quad (7)$$

The factor $f_m(r)$ is a function that gives the ratio of the neutron density $n_n(r)$ in relation to the electron density $n_e(r)$ at each radius of the solar interior, reads

$$f_m(r) = \frac{1}{2} \frac{n_n(r)}{n_e(r)}. \quad (8)$$

The variation of $V_m(r)$ (cf. equation 7) depends of the radial variation of neutrons as well as electrons inside the star. We notice, that in the particular case that $\theta_{14} = 0$, the 3 + 1 neutrino oscillation model becomes identical to the standard 3 neutrino oscillation model (for oscillations in vacuum and matter). Consequently, in this case $V_m(r)$ is reduced to a much simple expression (Bilenky, 2010): $V_m(r) = c_{13}^2 2E\sqrt{2}G_F n_e(r)/\Delta m_{21}^2$. These quantities (cf. equation 7) have a major impact on the formation of the sterile and electronic neutrino spectra. Figures 3 and 4 show the P_{ee} and P_{es} for the current standard solar model.

2.4 Emission of electron neutrino spectra from solar nuclear reactions

Since neutrinos are produced by nuclear reactions (either the PP chains and the CNO cycle) in different locations of the Sun's core, consequently, the survival probability of electron neutrinos will depend on the distance of the nuclear reaction to the center of the Sun (Lopes, 2013, 2017). This will also affect indirectly the probability of conversion of electron neutrinos into sterile neutrinos. The average probability $P_{ee,k}$ of electron neutrinos of energy E produced by a k nuclear reaction region is given by

$$P_{ee,k}(E) = A_k^{-1} \int_0^{R_\odot} P_{ee}(E, r) \phi_k(r) 4\pi\rho(r)r^2 dr, \quad (9)$$

where A_k is a normalization constant that is equal to $\int_0^{R_\odot} \phi_k(r) 4\pi\rho(r)r^2 dr$. $\phi_k(r)$ is the electron neutrino emission function for the following k nuclear reactions: pp , hep , 8B , 7Be , ${}^{13}N$, ${}^{15}O$ and ${}^{17}F$. In this study, we

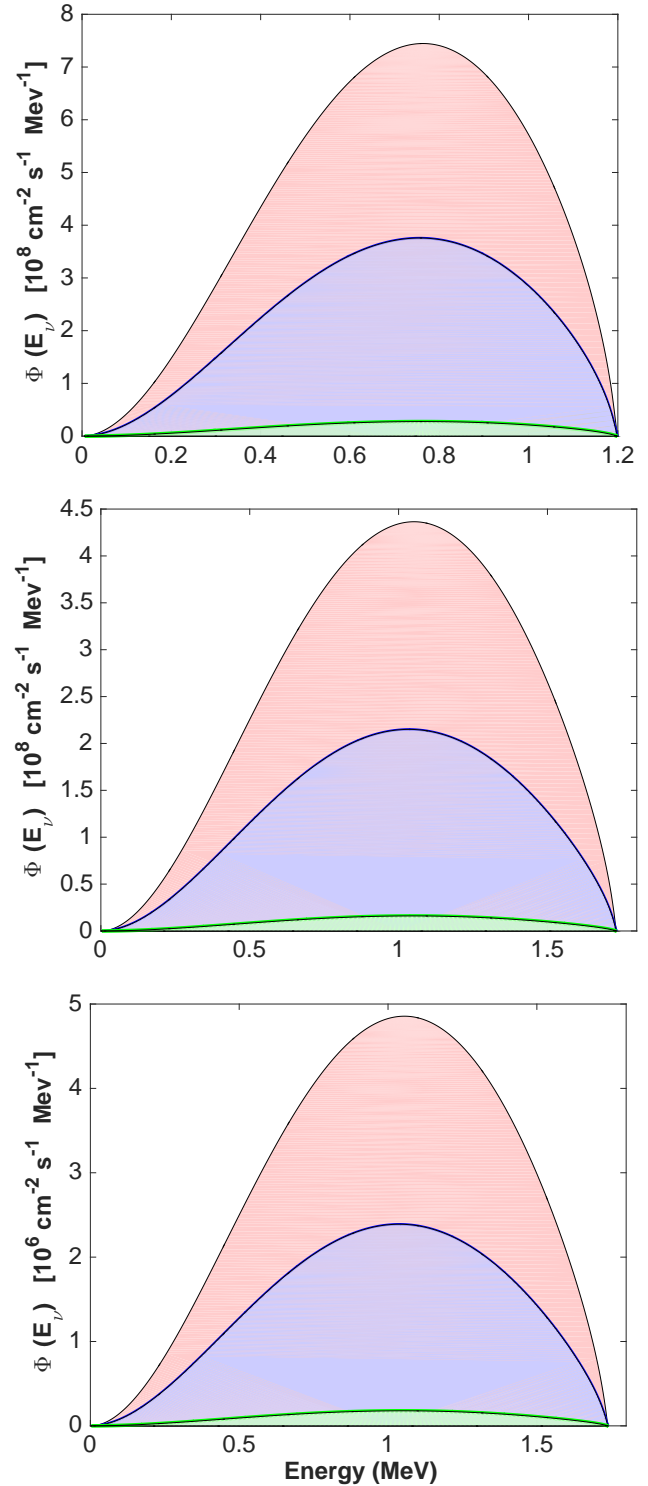


Fig. 9 The solar neutrino spectra for CNO neutrinos: Neutrino spectra of the *cno* nuclear reactions. $N13\nu$ (top), $O15\nu$ (middle) and $F17\nu$ (bottom). The colour scheme is the same used in Figure 5.

consider that all neutrinos produced in the solar nuclear reactions are of electron flavour as predicted by

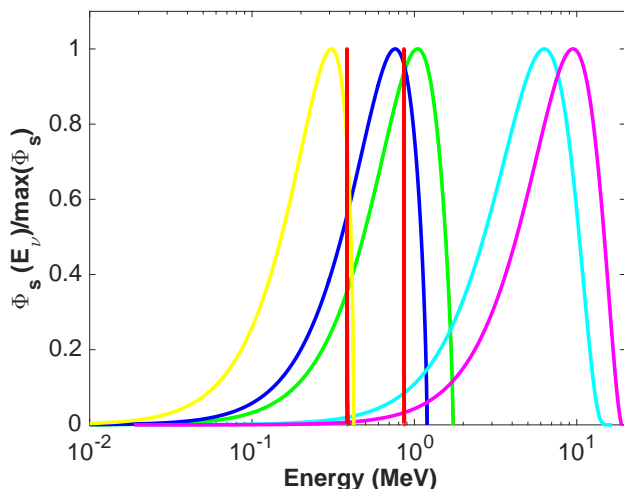


Fig. 10 Normalized sterile neutrino spectra for the Sun: pp (yellow curve), 8B (cyan curve), $Be7$ (red curve), hep (magenta curve), $N13$ (blue curve), $O15$ and $F17$ (green curve).

standard nuclear physics, therefore, the local density of neutrons only affects the $P_{ee,k}(E)$ by affecting the flavour of electron neutrinos due to the existence of a new sterile neutrino ν_s . It is important to note that $\phi_k(r)$, the neutrino source of each nuclear reaction, is sensitive to the local values (radius r) of the temperature, molecular weight, density, neutron and electronic densities.

In a 3+1 neutrino flavour oscillation model, as neutrinos propagate in the Sun's interior, the neutrino flavour oscillate between the four flavour states ν_e , ν_μ , ν_τ and ν_s either due to vacuum or matter oscillations. Although in outer space (between the Sun and the Earth) the flavour oscillations due to matter effects are expected to be small, the high density of the solar interior medium will enhance the scattering of neutrinos with other elementary particles, like electrons and neutrons leading to the increase of the probability of the neutrino oscillating between different flavour states. The particular distribution of electrons and neutrons in the solar interior leads to characteristic shapes of neutrino spectra (of electron neutrinos and sterile neutrinos) for each of the neutrino nuclear reactions occurring in the Sun's interior, as we will discuss in the next section (see figures: 5 – 9).

3 Prediction of the solar sterile and electron neutrino spectra

The spectrum of electron neutrinos from any specific nuclear reaction, like the β -decay processes occurring in the Sun's core are known to be essentially indepen-

Table 1 Solar neutrino sources of sterile neutrinos

Neut. source	Φ_t $\text{cm}^{-2}\text{s}^{-1}$	Φ_e $\text{cm}^{-2}\text{s}^{-1}$	Φ_s $\text{cm}^{-2}\text{s}^{-1}$
pp chain			
pp	$5.94 \cdot 10^{10}$	$3.09 \cdot 10^{10}$ (52%)	$2.22 \cdot 10^9$ (3.7%)
hep	$7.88 \cdot 10^3$	$2.88 \cdot 10^3$ (37%)	$2.64 \cdot 10^2$ (3.4%)
8B	$5.27 \cdot 10^6$	$1.91 \cdot 10^6$ (36%)	$1.76 \cdot 10^5$ (3.3%)
7Be 861.3 keV	$4.75 \cdot 10^9$	$2.38 \cdot 10^9$ (50%)	$1.76 \cdot 10^8$ (3.7%)
7Be 384.3 keV	$4.75 \cdot 10^9$	$2.44 \cdot 10^9$ (51%)	$1.77 \cdot 10^8$ (3.7%)
cno cycle			
${}^{13}N$	$5.32 \cdot 10^8$	$2.69 \cdot 10^8$ (51%)	$1.97 \cdot 10^7$ (3.7%)
${}^{15}O$	$4.49 \cdot 10^8$	$2.21 \cdot 10^8$ (49%)	$1.65 \cdot 10^7$ (3.7%)
${}^{17}F$	$5.01 \cdot 10^6$	$2.47 \cdot 10^6$ (49%)	$1.84 \cdot 10^5$ (3.7%)

The electronic neutrino fluxes (Φ_t) predicted for the current solar model as in reference Lopes & Silk (2013).

dent of the properties of the solar plasma. Actually, the neutrino spectrum emitted by these nuclear reactions occurring inside the Sun are identical to the same spectra emitted by the seminar nuclear reactions tested on many laboratories on Earth. Therefore, it is reasonable to assume that the neutrino emission spectra is the same in both cases (Lopes, 2017). Since the β -decay processes only produce electron neutrinos, using the theory of neutrino flavour oscillation is possible to predict in detail the spectrum shapes of sterile and electronic neutrinos arriving on Earth.

Here we make predictions of the sterile neutrino spectra of the main nuclear reactions occurring in the Sun, in the hope that this can be used as a guide for the future generation of neutrino detectors, which could help to establish (or rule out) the existence of sterile neutrinos. Once that the neutrinos emitted in the solar nuclear reactions are all of electron flavour ν_e , than the existence of other neutrino flavours in the solar neutrino spectrum (as it is possible to observe on solar neutrino detectors) is uniquely related with the nature of neutrino flavour oscillations, which leads to the convection of ν_e on other neutrino flavours: ν_μ , ν_τ and ν_s . Accordingly, the electron neutrino spectrum of the k nuclear reaction is defined as $\Phi_{k,t}(E)$ (with the subscript t referring to the emission electron neutrino spectrum of the nuclear reaction k), and $\Phi_{k,s\odot}(E)$ and $\Phi_{k,e\oplus}(E)$ are the sterile neutrino spectrum and the electron neutrino spectrum arriving on Earth. The function $\Phi_{k,t}(E)$ corresponds to the electron neutrino spectrum of a specific nuclear reaction computed theoretically, and also in many cases measured in the laboratory. The 8B neutrino spectrum is a very good example. The 8B neutrino spectrum (Bahcall & Holstein, 1986) has been shown to fit the experimental data with a high degree of accuracy (e.g., Winter et al., 2006). Hence, the sterile neutrino spectrum $\Phi_{k,s\odot}(E)$ is computed as

$$\Phi_{k,s\odot}(E) = P_{es,k}(E)\Phi_{k,t}(E), \quad (10)$$

where k is equal to one of the following values: pp , hep , 8B , 7Be , ${}^{13}N$, ${}^{15}O$ and ${}^{17}F$. Similarly the electron neutrino spectrum $\Phi_{k,e\odot}(E)$ is given by

$$\Phi_{k,e\odot}(E) = P_{ee,k}(E)\Phi_{k,t}(E). \quad (11)$$

Figures 5, 6, 7, 8 and 9 show the conversion of the emission neutrino spectra $\Phi_{k,t\odot}(E)$ in the two other spectrum flavours $\Phi_{k,e\odot}(E)$ and $\Phi_{k,s\odot}(E)$. Moreover, table 1 shows the total neutrino fluxes computed for the present-day standard solar model (Lopes & Silk, 2013). For each nuclear reaction, Φ_t is the total neutrino flux emitted by the nuclear reaction, and Φ_e and Φ_s correspond to the flux fractions of Φ_t that arrive at the solar detector as electron neutrinos or sterile neutrinos.

We start to notice that due to neutrino oscillations the electron neutrino spectra arriving on Earth detectors for all the solar nuclear reactions (considered in this study) are very different from the neutrino spectra emitted by the solar nuclear reactions (without neutrino oscillations). In particular, it is possible that the next generation of solar neutrino detectors will be able to measure $\Phi_{k,e\odot}(E)$. The sterile neutrino spectrum of all nuclear reactions have very small amplitudes and have identical spectral shapes although occurring at different neutrino energy ranges. In table 1 we show the predicted neutrino fluxes for the leading solar nuclear reactions for the current solar standard model as well as the predicted ratios of sterile neutrino fluxes and electronic neutrino fluxes. The small values of sterile neutrinos are due to the very small mixing angle θ_{14} . Only 4% of neutrinos arriving on Earth have a sterile flavour. This value is almost constant across all solar nuclear reactions. Nevertheless there is a small increase for the sterile neutrinos from the pp reaction and a small decrease for sterile neutrinos from the 8B reaction. This is a consequence of the fact that the pp and 8B nuclear reactions produce neutrinos with the smallest and the largest energies which due to the specific dependence sterile neutrino flavour oscillations with the local distribution of electrons and neutrons in the solar core leads to this specific variations. It is interesting to note that all sterile neutrinos in the solar neutrino spectrum have unique shapes related with the specific solar nuclear reactions on its origin. For instance, the two spectral lines of 7Be have strong asymmetry in their shape which could be helpful to look for hints related with sterile neutrinos in the solar neutrino spectrum. The strongest source of solar sterile neutrinos are the pp and 7Be nuclear reactions with a total flux of $2.22 \times 10^9 \text{ cm}^2\text{s}^{-1}$ and $1.76 \times 10^8 \text{ cm}^2\text{s}^{-1}$, followed by the ${}^{13}N$ and ${}^{15}O$ nuclear reactions with a total flux of $1.97 \times 10^7 \text{ cm}^2\text{s}^{-1}$ and $1.65 \times 10^7 \text{ cm}^2\text{s}^{-1}$ (cf. Table 1). Figure 11 shows the cumulative sterile neutrino spectrum coming from the

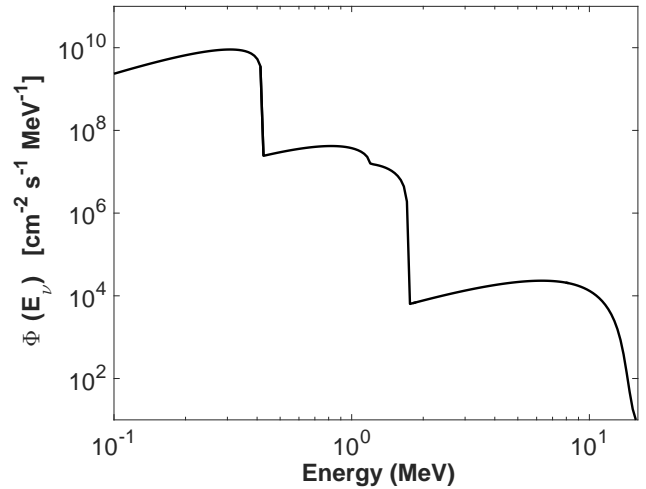


Fig. 11 The total sterile neutrino energy spectrum predicted by our standard solar model. The individual solar neutrino fluxes are shown in Table 1.

Sun. The maximum emission of sterile solar neutrinos corresponds to an energy of 0.307 MeV and a neutrino flux $9.0 \times 10^9 \text{ cm}^2\text{s}^{-1}$.

4 Conclusion

Sterile neutrinos are among the best candidates to resolve some of the leading problems in particle physics. At the same time these are very viable candidates to dark matter. Nevertheless, the hint of its existence has been questioned by a recent group of new experiments. The final proof beyond doubt of sterile neutrino existence will pass by its direct detection.

In this study we have computed for the first time the sterile spectrum of several key solar nuclear reactions. We found that from the solar neutrino flux arriving on Earth only 3% – 4% corresponds to sterile neutrinos. As expected, the strongest source is the pp nuclear reaction with a total flux of $2.22 \times 10^9 \text{ cm}^2\text{s}^{-1}$ followed by the 7Be nuclear reaction with a total flux one order of magnitude smaller. Equally, we have also predicted in detail the spectral shape of the sterile neutrino spectrum associated to the different solar nuclear reactions. In particular as shown in figure 10 the shape of these sterile neutrino spectra are quite distinct.

Final point: the Sun produces a significant amount of sterile neutrino on the spectral range from 10 KeV to 10 MeV, mostly coming for the pp nuclear reaction (in the neutrino energy range from 0.01 MeV up to 0.4 MeV), and 7Be (spectral lines 0.861 MeV and 0.384 MeV) that can affect experiments which are looking for relic (non-relativist) active and sterile neutrinos like

KATRIN and PTOLEMY Collaboration (Behrens et al., 2017; Betts et al., 2013). Indeed several experiments based in different principles have been proposed to detect such relic neutrinos (both components active and sterile neutrinos) (Cocco et al., 2008; Ando & Kusenko, 2010): electron-capture of decaying nuclei (Li & Xing, 2011b,a), annihilation of high-energy cosmic neutrinos at the Z-resonance, atomic de-excitation (Barenboim et al., 2005; Yoshimura et al., 2015) and neutrino capture using radioactive beta-decaying nuclei (Weinberg, 1962). The later seems to be the most promising technique with a few experiments already planned to that end like the KATRIN and PTOLEMY projects (Behrens et al., 2017; Dolde et al., 2017; Huang & Zhou, 2016; Betts et al., 2013). In an typical β -decay process like the one expected to be found in the PTOLEMY experiment, the relic neutrinos (cosmic neutrino background) will be shown as two independent kinks in the continuous β -spectrum, one due to the active neutrinos and a second small peak at higher energy associated to the admixture of sterile neutrinos (Long et al., 2014). The exact location of the energy peaks on the spectrum will depend on the masses of the active and sterile neutrinos.

In conclusion, we have computed the total flux of sterile neutrinos emitted by the Sun, as well as the solar sterile neutrino spectrum, this could be helpful in looking for sterile signatures by the next generation of solar neutrino detectors.

Acknowledgements The author thanks the Fundação para a Ciência e Tecnologia (FCT), Portugal, for the financial support to the Center for Astrophysics and Gravitation (CENTRA), Instituto Superior Técnico, Universidade de Lisboa, through the Grant No. UID/FIS/00099/201. Moreover, the author also acknowledges the support given by the Institut d’Astrophysique de Paris during his sabbatical visit.

References

- Abe, K., Haga, Y., Hayato, Y., et al. 2015, *Physical Review D*, **91**, 052019.
- Aguilar, A., Auerbach, L. B., Burman, R. L., et al. 2001, *Physical Review D*, **64**, 112007.
- Aguilar-Arevalo, A. A., Anderson, C. E., Brice, S. J., et al. 2010, *Physical Review Letters*, **105**, 181801.
- Aguilar-Arevalo, A. A., Brown, B. C., Bugel, L., et al. 2013, *Physical Review Letters*, **110**, 161801.
- Ando, S., & Kusenko, A. 2010, *Physical Review D*, **81**, 113006.
- Bahcall, J. N., & Holstein, B. R. 1986, *Physical Review C*, **33**, 2121.
- Barenboim, G., Requejo, O. M., & Quigg, C. 2005, *Physical Review D*, **71**, 083002.
- Behrens, J., Ranitzsch, P. C.-O., Beck, M., et al. 2017, *European Physical Journal C*, **77**, 410.
- Bergström, J., Gonzalez-Garcia, M. C., Maltoni, M., & Schwetz, T. 2015, *Journal of High Energy Physics*, **9**, 200.
- Betts, S., Blanchard, W. R., Carnevale, R. H., et al. 2013, [arXiv:1307.4738](https://arxiv.org/abs/1307.4738).
- Bilenky, S. 2010, *Lecture Notes in Physics*, Berlin Springer Verlag, 817.
- Billard, J., Strigari, L. E., & Figueroa-Feliciano, E. 2015, *Physical Review D*, **91**, 095023.
- Boyarsky, A., Iakubovskiy, D., & Ruchayskiy, O. 2012, *Physics of the Dark Universe*, **1**, 136.
- Cirelli, M., Marandella, G., Strumia, A., Vissani, F. 2005. *Nuclear Physics B* **708**, 215-267.
- Cocco, A. G., Mangano, G., & Messina, M. 2008, *Journal of Physics Conference Series*, **110**, 082014.
- Dolde, K., Mertens, S., Radford, D., et al. 2017, *Nuclear Instruments and Methods in Physics Research A*, **848**, 127.
- de Gouvêa, A., & Kelly, K. J. 2016, *Nuclear Physics B*, **908**, 318.
- Gonzalez-Garcia, M. C., Maltoni, M., & Schwetz, T. 2016, *Nuclear Physics B*, **908**, 199.
- Gonzalez-Garcia, M. C., Maltoni, M., & Schwetz, T. 2014, *Journal of High Energy Physics*, **11**, 52.
- Gonzalez-Garcia, M. C., & Maltoni, M. 2008, *Physics Reports*, **460**, 1.
- Giunti, C., & Laveder, M. 2011, *Physical Review C*, **83**, 065504.
- Giunti, C., Laveder, M., Li, Y. F., & Long, H. W. 2013, *Physical Review D*, **88**, 073008.
- de Holanda, P. C., & Smirnov, A. Y. 2004, *Physical Review D*, **69**, 113002.
- Huang, G.-y., & Zhou, S. 2016, *Physical Review D*, **94**, 116009.
- Aartsen, M. G., and 307 colleagues 2017. *Physical Review D* **95**, 112002.
- Li, Y. F., & Xing, Z.-Z. 2011, *Physics Letters B*, **695**, 205.
- Li, Y. F., & Xing, Z.-z. 2011, *Journal of Cosmology and Astroparticle Physics*, **8**, 006.
- Long, A. J., Lunardini, C., & Sabancilar, E. 2014, *Journal of Cosmology and Astroparticle Physics*, **8**, 038.
- Lopes, I. 2017, *Physical Review D*, **95**, 015023 *Physical Review D*, **95**, 015023.
- Lopes, I. 2013, *Physical Review D*, **88**, 045006.
- Lopes, I., & Silk, J. 2013, *Monthly Notices of the Royal Astronomical Society*, **435**, 2109.
- Lopes, I., & Turck-Chièze, S. 2013, *The Astrophysical Journal*, **765**, 14.

-
- Adhikari, R., Agostini, M., Ky, N. A., et al. 2017, *Journal of Cosmology and Astroparticle Physics*, **1**, 025.
- Ko, Y. J., Kim, B. R., Kim, J. Y., et al. 2017, *Physical Review Letters*, **118**, 121802.
- Kopp, J., Machado, P. A. N., Maltoni, M., & Schwetz, T. 2013, *Journal of High Energy Physics*, **5**, 50.
- Kuo, T. K., Pantaleone, J. 1989. *Reviews of Modern Physics* **61**, 937-980.
- Maltoni, M., & Smirnov, A. Y. 2016, *European Physical Journal A*, **52**, 87.
- Minkowski, P. 1977, *Physics Letters B*, **67**, 421.
- Maki, Z., Nakagawa, M., & Sakata, S. 1962, *Progress of Theoretical Physics*, **28**, 870.
- Mention, G., Fechner, M., Lasserre, T., et al. 2011, *Physical Review D*, **83**, 073006.
- Palazzo, A. 2011, *Physical Review D*, **83**, 113013.
- Serenelli, A. M., Haxton, W. C., & Peña-Garay, C. 2011, *The Astrophysical Journal*, **743**, 24.
- Shrock, R. E. 1980, *Physics Letters B*, **96**, 159.
- Turck-Chièze, S., Palacios, A., Marques, J. P., & Nghiem, P. A. P. 2010, *The Astrophysical Journal*, **715**, 1539.
- Weinberg, S. 1962, *Physical Review*, **128**, 1457.
- Yoshimura, M., Sasao, N., & Tanaka, M. 2015, *Physical Review D*, **91**, 063516.
- Winter, W. T., Freedman, S. J., Rehm, K. E., & Schiffer, J. P. 2006, *Physical Review C*, **73**, 025503.
- Wolfenstein, L. 1978, *Physical Review D*, **17**, 2369.